



Unsteady Heat and Mass Transfer Near the Stagnation-point on a Vertical Permeable Surface: a Comprehensive Report of Dual Solutions

H. Tamim, A. Abbassi*

Department of Mechanical Engineering, Amirkabir University of Technology, Tehran, Iran

PAPER INFO

Paper history:

Received 22 February 2013

Accepted in revised form 18 September 2014

Keywords:

Unsteady Flow
Double Diffusive Convection
Stagnation-point Flow
Mixed Convection
Dual Solutions
Vertical Surface
Suction/Injection

ABSTRACT

In this paper, the problem of unsteady mixed convection boundary layer flow of a viscous incompressible fluid near the stagnation-point on a vertical permeable plate with both cases of prescribed wall temperature and prescribed wall heat flux is investigated numerically. Here, both assisting and opposing buoyancy forces are considered and studied. The nonlinear coupled partial differential equations governing the flow, thermal and concentration fields are first transformed into a set of nonlinear coupled ordinary differential equations by a set of suitable similarity transformations. The resulting system of coupled nonlinear ordinary differential equations is solved numerically using the Runge-Kutta scheme coupled with a conventional shooting procedure. Numerical results are obtained for the skin-friction coefficient, Nusselt number and Sherwood number as well as for the velocity, temperature and concentration profiles for some values of the governing parameters, namely, the unsteadiness parameter A , permeability parameter f_0 and mixed convection parameter λ . It is found that dual solutions exist for both assisting and opposing flows, and the range of the mixed convection parameter for which the solution exists, increases with suction and unsteadiness parameters.

doi: 10.5829/idosi.ije.2015.28.05b.16

NOMENCLATURE

A	Unsteadiness parameter	x, y	Velocity component
C	Fluid concentration	u, v	Cartesian coordinates
C_f	Skin friction coefficient	Greek Symbols	
D	Mass diffusivity	α	Thermal diffusivity
f	Dimensionless stream function	β	Volumetric thermal expansion coefficient
g	Acceleration due to gravity	γ	Constant
Gr	Grashof number	$\phi(\eta)$	Dimensionless concentration
k	Thermal conductivity of the fluid	η	Similarity variable
L	Characteristic length	$\theta(\eta)$	Dimensionless temperature
N	Ratio of buoyancy forces	λ	Buoyancy or mixed convection parameter
Nu_x	Local Nusselt number	ν	Kinematic viscosity
Pr	Prandtl number	ρ	Fluid density
P	Pressure	τ	Shear stress
q_w	Surface heat flux	ψ	Stream function
Re	Reynolds number	Subscripts	
Sc	Schmidt number	W	Condition at the surface of the plate
Sh_x	Local Sherwood number	∞	Ambient condition
s_w	Surface mass flux	e	Inviscid flow
T	Fluid temperature	Subscripts Gas	
u_e	Inviscid flow velocity	'	Differentiation with respect to η

*Corresponding Author's Email: abbassi@aut.ac.ir (A. Abbassi)

Please cite this article as: H. Tamim, A. Abbassi, Unsteady Heat and Mass Transfer Near the Stagnation-point on a Vertical Permeable Surface: a Comprehensive Report of Dual Solutions, International Journal of Engineering (IJE), TRANSACTIONS B: Applications Vol. 28, No. 5, (May 2015) 771-780

1. INTRODUCTION

Progress in modern technologies has played an important role in interesting researchers in fluid flows which include interaction between various phenomena. Free convection is caused by the temperature difference of fluid at different locations and forced convection is the flow of heat due to some external applied forces. The characteristics of a mixed convection boundary layer depend on the velocity of the forced stream, the thermal and concentration conditions at the wall.

It is worth mentioning that mixed convection flows have many applications; hence, they have great importance. They can be observed in natural phenomena and engineering devices such as atmospheric boundary layer flows, heat exchangers, solar collectors, nuclear reactors and electronic equipment, and so on. In such cases, finding similar solutions may be directly usable in technical applications or may provide a standard tool for calculating approximately more complex non-similar cases.

The basic studies on similarity solution for the thermal boundary layer over flat surfaces are presented in heat transfer text books, namely, Bejan [1] and Incropera et al. [2]. Bejan [1] has suggested a similarity temperature variable which reduced the energy equation to an ordinary differential equation. Also, various studies [3, 4] have presented different variations of temperature and heat flux at the plate. Risbeck et al. [5] studied mixed convection flow over a horizontal flat plate using a single mixed convection parameter that covers the entire regime of mixed convection. Datta et al. [6] obtained non-similar solution of a steady mixed convection flow over horizontal flat plate with surface mass transfer. Ishak et al. [7] have studied the mixed convection boundary layer flow past an isothermal horizontal plate. Rahmannedhad et al. [8] investigated the effects of magnetic field on mixed convection flow, and the effects of Reynolds number and fluid temperature were studied by Rostamzadeh et al. [9].

The existence of non-unique (dual) similarity solutions in mixed convection boundary layer flow has been pointed out by many researchers, for example, de Hoog et al. [10], Afzal and Hussain [11], Ramachandran et al. [12], Ridha [13] and Lok et al. [14]. Ramachandran et al. [12] studied the steady laminar mixed convection in two-dimensional stagnation flows around vertical surfaces by considering both cases of an arbitrary wall temperature and arbitrary surface heat flux variations. They found that a reverse flow develops in the buoyancy opposing flow region, and dual solutions are found to exist for a certain range of the buoyancy parameter. Dual solutions were found to exist by these authors only for the opposing flow case. The existence of dual solutions for both assisting and opposing flows

was reported by Ridha [13] when he reconsidered the problems of mixed convection flow over a horizontal surface, mixed convection flow over a vertical surface, and axisymmetric mixed convection flow which has been investigated previously by some authors. Ridha [13] pointed out that the failure of the previous investigations to report the existence of dual solutions only for the assisting flow is perhaps due to the misleading behavior of the non-dimensional temperature used in the similarity formulation. Later, Deswita et al. [15] extended the work by Ridha [13] to obtain dual similarity solutions for the case when the horizontal surface of the wedge is permeable (porous).

It may be noted that, on a different approach, Merrill et al. [16] have performed a stability analysis for different steady state solutions of mixed convection flow on a vertical surface near the stagnation point. They have reported the existence of dual solutions where the upper branch are linearly stable while those of lower branch are linearly unstable. It is worthy to mention that Ridha [13], Ishak et al. [17, 18] and Subhashini et al. [19, 20] have reported in their respective studies that the upper branch solution are most physically relevant solutions whereas the lower branch solution seem to deprive physical significance or may have realistic meaning in different situations. According to the studies by Merkin [21], Harris et al. [22], and Postelnicu and Pop [23], the first solutions are physically realizable, while the second solutions are not.

Unsteady boundary layer plays important roles in many engineering problems like start-up process and periodic fluid motion. Unsteady boundary layer has different behavior due to extra time-dependent terms, which will influence the fluid motion pattern and the boundary layer separation [24]. Some typical examples of unsteady boundary layers in the history of fluid mechanics are the Rayleigh problem and Stokes oscillating plate [25, 26]. Yang [27] investigated the unsteady boundary layer for a stagnation flow involving the starting up of a cylinder. Following the pioneer work by Yang [27] the problem was extended to oblique stagnation-point flow by Wang [28]. Rahimi and Jalali [29] studied unsteady free convection from a sphere, and Jabari Moghadam and Baradaran Rahimi [30] studied time-dependent behavior of flow between two rotating spheres. Also, Haghighi and Rahimi [31] investigated the effects of unsteadiness on axisymmetric stagnation-point flow and heat transfer. Recently, the boundary layers of an unsteady stagnation-point flow in a nanofluid was considered by Bachok et al. [32] and found dual solutions for negative values of the unsteadiness parameters.

It may be remarked that many of earlier studies did not include the effect of mass diffusion. However, if the body surface and the free stream fluid temperature differ, not only energy will be transferred to the flow

but also density difference exists. When heat and mass diffusion occurs simultaneously, it leads to a complex fluid motion called double diffusive convection. In practice, double diffusive convection may appear in wide range of scientific fields such as oceanography, astrophysics, geology, biology, chemical processes, etc. This fact motivates the authors to investigate the combined effects of thermal and mass diffusion on mixed convection flow.

Recently, Rohni et al. [33] have studied the unsteady mixed convection boundary-layer flow near the two-dimensional stagnation point on a vertical permeable surface embedded in a fluid-saturated porous medium with suction and temperature slip effect. Their results show that multiple solution exist for a certain range of governing parameters. The aim of the present paper is to study the simultaneous influence of unsteady double diffusive mixed convection flow near stagnation-point on a vertical permeable surface.

2. MATHEMATICAL FORMULATION

Consider a two-dimensional laminar viscous and incompressible stagnation-point flow of an unsteady flow with a velocity of the outer or inviscid flow of the form $u_e(x,t) = U_\infty(x/L)(1-\gamma t)^{-1}$, where γ is a positive constant. We select a coordinate frame in which x-axis is extending along the surface, while the y-axis is measured normal to the surface of the plate and is positive in the direction from the surface to the fluid. Both cases of prescribed wall temperature (case A) and prescribed wall heat flux (case B) are considered and studied. The plate is maintained at a temperature $T_w(x,t)$ for case A (see Figure 1) and it is heated by a heat flux $q_w(x,t)$ for case B (Figure 2). Also, the concentration near the wall is $C_w(x,t)$.

Variations in temperature and concentration of fluid make buoyancy forces. In order to relate the density changes to the above parameters (temperature and concentration) and couple them to the flow field, Boussinesq approximation is used for representing fluid properties. Under these assumptions and boundary layer approximations, the system of equations which models the problem under consideration, is given by:

$$\frac{\partial u}{\partial x} + \frac{\partial v}{\partial y} = 0 \tag{1}$$

$$\frac{\partial u}{\partial t} + u \frac{\partial u}{\partial x} + v \frac{\partial u}{\partial y} = -\frac{1}{\rho_\infty} \frac{\partial p}{\partial x} + \nu \frac{\partial^2 u}{\partial y^2} + g\beta(T - T_\infty) + g\beta^*(C - C_\infty) \tag{2}$$

$$\frac{\partial T}{\partial t} + u \frac{\partial T}{\partial x} + v \frac{\partial T}{\partial y} = \alpha \frac{\partial^2 T}{\partial y^2} \tag{3}$$

$$\frac{\partial C}{\partial t} + u \frac{\partial C}{\partial x} + v \frac{\partial C}{\partial y} = D \frac{\partial^2 C}{\partial y^2} \tag{4}$$

with the initial and boundary conditions:

$$t < 0: \quad u = v = 0, \quad T = T_\infty, \quad C = C_\infty \quad \text{for any } x, y$$

$$t \geq 0: \quad \begin{cases} u = 0, \quad v = V_w(x, t), \quad T = T_w(x, t), \\ C = C_w(x, t) \quad \text{at } y = 0 \text{ (for case A)} \\ u = 0, \quad v = V_w(x, t), \quad -k\partial T / \partial y = q_w(x, t), \\ C = C_w(x, t) \quad \text{at } y = 0 \text{ (for case B)} \\ u \rightarrow u_e(x, t), \quad T \rightarrow T_\infty, \quad C \rightarrow C_\infty \quad \text{as } y \rightarrow \infty \end{cases} \tag{5}$$

Here u and v are the velocity components along the x and y axes, respectively, T and C the fluid temperature and fluid concentration, respectively, α the thermal diffusivity, D the mass diffusivity, β and β^* volumetric coefficient of thermal expansion and coefficient of expansion for concentration, respectively, and g the acceleration due to gravity. Further, $V_w(x,t)$ is the surface mass flux, where $V_w(x,t) < 0$ corresponds to velocity suction and $V_w(x,t) > 0$ corresponds to velocity blowing or injection, respectively.

By employing momentum equation in direction of y -axis and Bernoulli's equation, in free stream, we have

$$\frac{\partial p}{\partial y} = 0 \tag{6}$$

$$-\frac{1}{\rho_\infty} \frac{\partial p}{\partial x} = -\frac{1}{\rho_\infty} \frac{dp}{dx} = -\frac{1}{\rho_\infty} \frac{dp_\infty}{dx} = \frac{\partial u_e}{\partial t} + u_e \frac{\partial u_e}{\partial x} \tag{7}$$

Using Equation (7), Equation (2) can be written as:

$$\frac{\partial u}{\partial t} + u \frac{\partial u}{\partial x} + v \frac{\partial u}{\partial y} = \frac{\partial u_e}{\partial t} + u_e \frac{\partial u_e}{\partial x} + \nu \frac{\partial^2 u}{\partial y^2} + g\beta(T - T_\infty) + g\beta^*(C - C_\infty) \tag{8}$$

In order to obtain similarity solutions, $u_e(x,t)$, $T_w(x,t)$, $q_w(x,t)$ and $C_w(x,t)$ are assigned in the following form:

$$u_e(x, t) = U_\infty \left(\frac{x}{L}\right) \left(\frac{1}{1-\gamma t}\right)$$

$$T_w(x, t) = T_\infty + \Delta T \left(\frac{x}{L}\right)^2 \left(\frac{1}{1-\gamma t}\right)^2 \quad \text{(for case A)}$$

$$q_w(x, t) = k\Delta T \left(\frac{x}{L}\right)^2 \left(\frac{U_\infty}{\nu L}\right)^{1/2} \left(\frac{1}{1-\gamma t}\right)^{5/2} \quad \text{(for case B)}$$

$$C_w(x, t) = C_\infty + \Delta C \left(\frac{x}{L}\right)^2 \left(\frac{1}{1-\gamma t}\right)^2 \tag{9}$$

where, U_∞ and γ are constants, k is thermal conductivity, L a characteristic length, ΔT and ΔC denote scale temperature and scale concentration, respectively. For both cases, the assisting flow ($\Delta T > 0$) occurs if the upper half of the plate is heated while the

lower half of the plate is cooled. In this case, the flows near the heated and cooled plates tend to move upward and downward, respectively. Therefore, this behavior acts to assist the flow field. The opposing flow ($\Delta T < 0$) occurs if the upper part of the plate is cooled while its lower part is heated. We now introduce the following similarity transformations:

$$\eta = \left(\frac{U_\infty}{\nu L (1 - \gamma t)} \right)^{1/2} y, \quad \psi = \left(\frac{U_\infty \nu L}{(1 - \gamma t)} \right)^{1/2} \left(\frac{x}{L} \right) f(\eta)$$

$$T - T_\infty = \Delta T \left(\frac{x}{L (1 - \gamma t)} \right)^2 \theta(\eta) \tag{10}$$

$$C - C_\infty = \Delta C \left(\frac{x}{L (1 - \gamma t)} \right)^2 \phi(\eta)$$

where, ψ is the stream function defined as $u = \partial\psi/\partial y$ and $v = -\partial\psi/\partial x$, so as to identically satisfy Equation (1); and the velocity components u and v are obtained as:

$$u = U_\infty \left(\frac{x}{L} \right) (1 - \gamma t)^{-1} f'(\eta) = u_e(x, t) f'(\eta) \tag{11}$$

$$v = - \left(\frac{U_\infty \nu}{L (1 - \gamma t)} \right)^{1/2} f(\eta) \tag{12}$$

where, primes denote differentiation with respect to η . Therefore, in order that similarity solutions of Equations (1-5) exist, we take:

$$v_w(t) = - \left(\frac{U_\infty \nu}{L (1 - \gamma t)} \right)^{1/2} f_0 \tag{13}$$

where the dimensionless constant f_0 determines the transpiration rate, with $f_0 > 0$ for suction, $f_0 < 0$ for injection and $f_0 = 0$ for an impermeable surface. Employing the similarity transformations (10), Equations (3), (4) and (8) reduce to the following nonlinear ordinary differential equations:

$$f''' + ff'' - f'^2 + 1 + A \left(1 - f' - \frac{\eta}{2} f'' \right) + \lambda (\theta + N\phi) = 0 \tag{14}$$

$$\frac{1}{Pr} \theta'' + f\theta' - 2f\theta - A \left(2\theta + \frac{\eta}{2} \theta' \right) = 0 \tag{15}$$

$$\frac{1}{Sc} \phi'' + f\phi' - 2f\phi - A \left(2\phi + \frac{\eta}{2} \phi' \right) = 0 \tag{16}$$

subject to the transformed boundary conditions:

$$f(0) = f_0, \quad f'(0) = 0, \quad \theta(0) = 1, \quad \phi(0) = 1$$

$$f'(\infty) \rightarrow 1, \quad \theta(\infty) \rightarrow 0, \quad \phi(\infty) \rightarrow 0 \quad (\text{for case A}) \tag{17}$$

$$f(0) = f_0, \quad f'(0) = 0, \quad \theta'(0) = -1, \quad \phi(0) = 1$$

$$f'(\infty) \rightarrow 1, \quad \theta(\infty) \rightarrow 0, \quad \phi(\infty) \rightarrow 0 \quad (\text{for case B})$$

Where, A is the unsteadiness parameter, $Pr = \nu/\alpha$ is the

Prandtl number, $Sc = \nu/D$ is the Schmidt number, λ is the buoyancy or mixed convection parameter and the ration of buoyancy forces N are given by:

$$A = \frac{\gamma L}{U_\infty}, \quad \lambda = \frac{Gr}{Re^{5/2}}, \quad N = \frac{Gr^*}{Gr}$$

$$Gr = \frac{g\beta\Delta TL^3}{\nu^2 (1 - \gamma t)^2}, \quad Gr^* = \frac{g\beta^* \Delta CL^3}{\nu^2 (1 - \gamma t)^2}, \quad Re = \frac{U_\infty L}{\nu (1 - \gamma t)} \tag{18}$$

with Gr and Gr^* being the Grashof numbers and Re is the Reynolds number. It should be noticed that $\lambda > 0$ for assisting flow, $\lambda < 0$ for opposing flow and $\lambda = 0$ for forced convection flow. The physical quantities of interest are the skin friction coefficient C_f , the local Nusselt number Nu_x and the local Sherwood number Sh_x , which are defined by:

$$C_f = \frac{\tau_w}{\rho u_e^2}, \quad Nu_x = \frac{xq_w}{k(T_w - T_\infty)}, \quad Sh_x = \frac{xs_w}{D(C_w - C_\infty)} \tag{19}$$

where, the wall shear stress τ_w , the wall heat flux q_w and the wall mass flux s_w are given by:

$$\tau_w = \mu \left(\frac{\partial u}{\partial y} \right)_{y=0}, \quad q_w = -k \left(\frac{\partial T}{\partial y} \right)_{y=0}, \quad s_w = -D \left(\frac{\partial C}{\partial y} \right)_{y=0} \tag{20}$$

so we have:

$$C_f = \frac{\tau_w}{\rho u_e^2} = \frac{\mu \left(\frac{\partial u}{\partial y} \right)_{y=0}}{\rho u_e^2}$$

$$Nu_x = \frac{-xk \left(\frac{\partial T}{\partial y} \right)_{y=0}}{k(T_w - T_\infty)}, \quad Sh_x = \frac{-xD \left(\frac{\partial C}{\partial y} \right)_{y=0}}{D(C_w - C_\infty)} \tag{21}$$

with μ and D being the dynamic viscosity and mass diffusivity, respectively. Using the similarity variables (10), we obtain:

$$\left(Re_x^{1/2} \right) C_f = f''(0)$$

$$\left(Re_x^{-1/2} \right) Nu_x = -\theta'(0), \quad \left(Re_x^{-1/2} \right) Sh_x = -\phi'(0) \tag{22}$$

where, $Re_x = u_e(x, t) x / \nu$ is the local Reynolds number.

3. RESULTS AND DISCUSSIONS

The nonlinear ordinary differential Equations (14-16) subject to the boundary conditions (17) have been solved numerically for different values of the governing parameters A , f_0 , λ , Pr and Sc using fourth order Runge–Kutta scheme coupled with a conventional shooting procedure. The values of the dimensionless skin friction coefficient $f''(0)$, local Sherwood number $-\phi'(0)$ and local Nusselt number $-\theta'(0)$ (for case A) and dimensionless wall temperature $\theta(0)$ (for case B)

obtained and compared with previously reported cases. This comparison is shown in Table 1. It is seen that the present values of $f''(0)$ are in very good agreement with the results obtained by Ramachandran et al. [12], Lok et al. [14] and Ishak et al. [34]. Therefore, it can be concluded that the developed code can be used with great confidence to study the problem discussed in this

paper. Also, the values of $f'(0)$, $-\phi'(0)$ and $-\theta'(0)$ (for case A) and $\theta(0)$ (for case B) are presented in Tables 2-4 for some particular cases, respectively. The results show that increasing in unsteadiness parameter and suction parameter increase the dimensionless skin friction coefficient, dimensionless Sherwood and Nusselt numbers in first solution for case A.



Figure 1. Physical model of two-dimensional stagnation point flow on a vertical surface for prescribed wall temperature case.

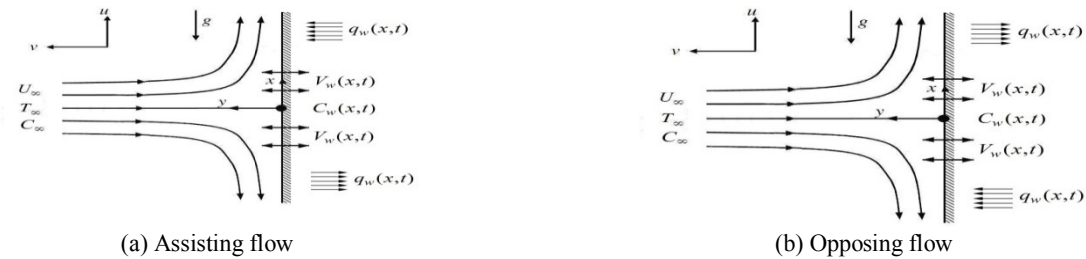


Figure 2. Physical model of two-dimensional stagnation point flow on a vertical surface for prescribed wall heat flux case.

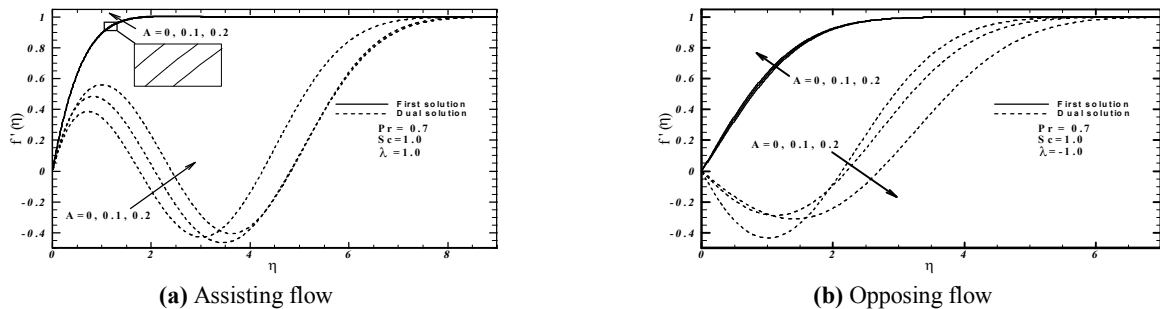


Figure 3. Velocity profiles $f'(\eta)$ for different unsteadiness parameter A when $Pr = 0.7$, $Sc=1.0$, $N=0.2$ (case A)

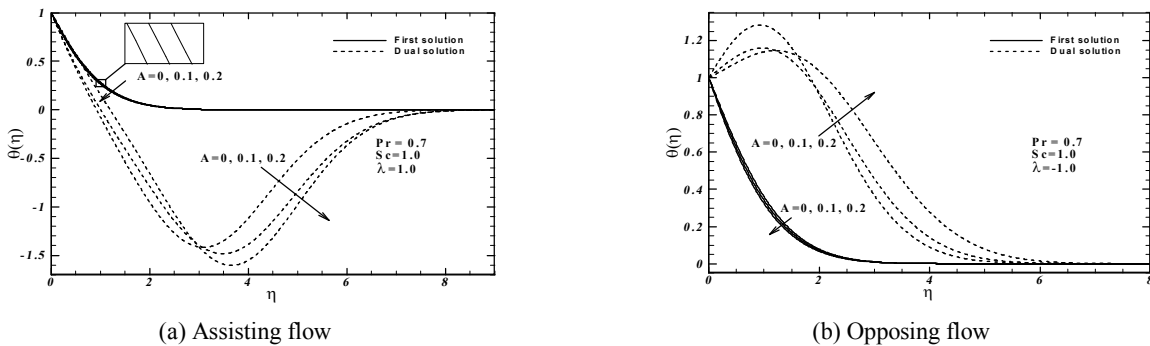
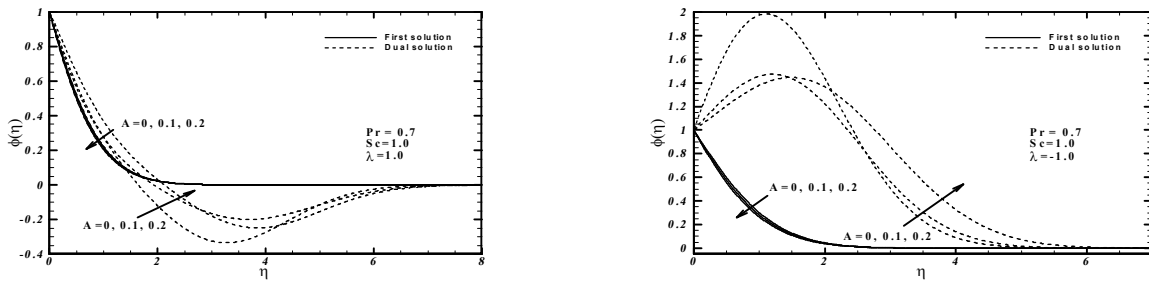


Figure 4. Temperature profiles $\theta(\eta)$ for different unsteadiness parameter A when $Pr = 0.7$, $Sc=1.0$, $N=0.2$ (case A)



(a) Assisting flow

(b) Opposing flow

Figure 5. Concentration profiles $\phi(\eta)$ for different unsteadiness parameter A when $Pr = 0.7$, $Sc=1.0$, $N=0.2$ (case A).

TABLE 1. Values of $f'(0)$ for various values of Pr when $A=0$, $N=0$ and $f_0=0$ (case A).

Pr	Ramachandran et al. [12]		Lok et al. [14]		Ishak et al. [19]		Present results	
	$\lambda = -1$	$\lambda = 1$	$\lambda = -1$	$\lambda = 1$	$\lambda = -1$	$\lambda = 1$	$\lambda = -1$	$\lambda = 1$
0.7	0.6917	1.7063	0.691693	1.706376	0.6917	1.7063	0.6917	1.7063
7	0.9235	1.5179	0.923528	1.517952	0.9235	1.5179	0.9235	1.5179
20	1.0031	1.4485	1.003158	1.448520	1.0031	1.4485	1.0031	1.4485
40	1.0459	1.4101	1.045989	1.410094	1.0459	1.4101	1.0459	1.4101
60	1.0677	1.3903	1.067703	1.390311	1.0677	1.3903	1.0677	1.3903
80	1.0817	1.3774	1.081719	1.377429	1.0817	1.3774	1.0817	1.3774
100	1.0918	1.3680	1.091840	1.368070	1.0918	1.3680	1.0918	1.3680

TABLE 2. Values of $f'(0)$ for various values of A , f_0 and λ when, $Pr = 0.7$ and $N=0.2$.

A	f_0	$\lambda = 1$				$\lambda = -1$			
		First solution		Second solution		First solution		Second solution	
		Case A	Case B	Case A	Case B	Case A	Case B	Case A	Case B
0	0	1.7472	1.7789	1.2009	-0.3166	0.6372	0.3746	-0.4467	-0.3677
0.1		1.7608	1.7700	1.3521	-0.2213	0.6922	0.5533	-0.3653	-0.5930
0.2		1.7749	1.7649	1.4013	-0.1205	0.7437	0.6723	-0.2841	0.7329
0	-0.5	1.4895	1.6280	1.2214	-0.2215	0.3322	-	-0.2383	-
	.5	2.0380	1.9870	0.8426	-0.8233	0.9919	1.2884	-0.8124	-1.1523

TABLE 3. Values of $-\phi'(0)$ for various values of A , f_0 and λ when, $Pr = 0.7$ and $N=0.2$.

A	f_0	$\lambda = 1$				$\lambda = -1$			
		First solution		Second solution		First solution		Second solution	
		Case A	Case B	Case A	Case B	Case A	Case B	Case A	Case B
0	0	1.0589	1.0639	0.9027	-3.2253	0.8490	0.7814	-0.6073	0.4792
0.1		1.1238	1.1252	0.9919	-2.5782	0.9380	0.9073	-0.3883	0.4373
0.2		1.1866	1.1852	1.0582	-0.5512	1.0208	1.0068	-0.2312	0.4252
0	-0.5	0.7852	0.8093	0.6853	-2.1233	0.5127	-	-0.2002	-
	.5	1.3786	1.3721	1.2135	-4.2568	1.2216	1.2709	-1.5918	0.3925

TABLE 4. Values of $-\theta'(0)$ (case A) and $\theta(0)$ (case B) for various values of A , f_0 and λ when, $Pr = 0.7$ and $N=0.2$.

A	f_0	$\lambda = 1$				$\lambda = -1$			
		First solution		Second solution		First solution		Second solution	
		Case A	Case B	Case A	Case B	Case A	Case B	Case A	Case B
0	0	0.9241	1.0772	1.1851	-1.1604	0.7497	1.4411	-0.2550	2.2240
0.1		0.9765	1.0229	1.1665	-0.9134	0.8209	1.2573	-0.1465	2.4269
0.2		1.0273	0.9746	1.1234	-0.7513	0.8875	1.1418	-0.0522	2.5256
0	-0.5	0.7246	1.3422	0.8400	-0.9642	0.4939	-	-0.0944	-
	.5	1.1495	0.8743	1.7331	-1.2241	1.0187	0.9438	-0.5207	3.2312

It is also evident from these Tables that the dimensionless skin friction coefficient and the dimensionless Sherwood number increase while the dimensionless wall temperature decreases when the suction parameter increases.

Figures 3, 4 and 5 respectively show the effects of unsteadiness parameter A on velocity, temperature and concentration profiles for $Pr = 0.7$, $Sc=1.0$, $N=0.2$ and $f_0=0$ for case A. These figures show that the unsteadiness increases the velocity profiles while decreases the temperature and concentration profiles for first solutions. Also, it is seen from these figures that, increasing the unsteadiness parameter increases the velocity, thermal and concentration boundary layer thicknesses for second solutions. The velocity gradient at the wall is positive for both solutions range in the assisting flow; besides it is negative for second solution in the opposing flow case. Again, from this observation we can see that the temperature profiles are negatives for the second solutions in assisting flow case, away from the wall ($\eta=0$). As discussed by Ridha [13], those solutions for which $\theta(\eta) < 0$ for any η have no physical sense. This can be explained by using the definition of the dimensionless temperature $\theta(\eta)$ given in 10, that requires T must be less than the ambient temperature T_∞ to give $\theta(\eta) < 0$, since $T_w > T_\infty$ for assisting flow (heated plate). The variations of $f''(0)$, $-\theta'(0)$ and $-\phi'(0)$ with buoyancy parameter λ for $Pr = 0.7$, $Sc=1.0$, $N=0.2$, and some values of A are shown in Figures 6, 7 and 8 respectively, all for $f_0=0$. It is observed that the mixed

convection parameter for which the solution exists increases with unsteadiness parameter and it is possible as well to obtain dual solutions for the similarity Equations (14-17) for assisting flow ($\lambda > 0$), apart from those for opposing flow ($\lambda < 0$) that have been reported by Ramachandran et al. [10] and Lok et al. [14]. For assisting flow ($\lambda > 0$), there is a favorable pressure gradient due to the buoyancy forces, which results in the flow being accelerated, and consequently, there is a larger skin friction coefficient than in the non-buoyant case ($\lambda=0$) as well as the opposing flow case ($\lambda < 0$). It is seen that the solution exists up to a critical value of λ (say λ_c) with two solution branches for $\lambda > \lambda_c$, a saddle-node bifurcation at $\lambda = \lambda_c$ and no solutions for $\lambda < \lambda_c$. We expect the first solution to be stable, while the second solution not, since the first solution is the only solution for the case $\lambda=0$, and the existence of reverse flow region for the second solution. On the other hand, Figure 4-b illustrates for the second solution of the temperature the existence of the heat generation inside the boundary layer, which is not physically possible while the viscous dissipation effects has not been considered in the present physical model. Figures 9, 10 and 11 illustrate the variations of $f''(0)$, $\theta(0)$ and $-\phi'(0)$ with buoyancy parameter λ for $Pr = 0.7$, $Sc=1.0$, $N=0.2$ and some values of A for case B. Similar to the figures of case A, unsteadiness parameter increases the range of mixed convection parameter for which the solution exists, and we can see that there are two solutions for $\lambda_c < \lambda \neq 0$ while there is only one for $\lambda = \lambda_c$ and $\lambda = 0$.

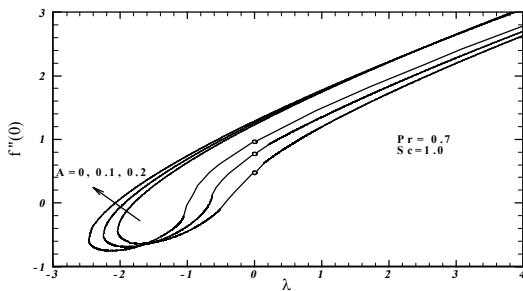


Figure 6. Variation of $f''(0)$ with λ for different unsteadiness parameter A when $N=0.2$, $Pr = 0.7$, $Sc=1.0$ and case A.

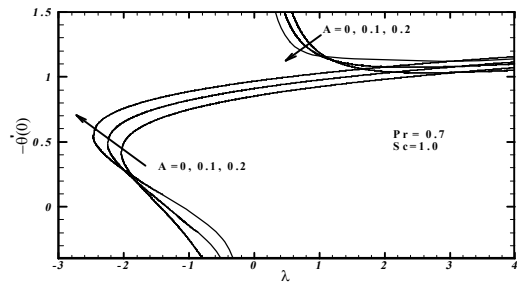


Figure 7. Variation of $-\theta'(0)$ with λ for different unsteadiness parameter A when $N=0.2$, $Pr = 0.7$, $Sc=1.0$ and case A.

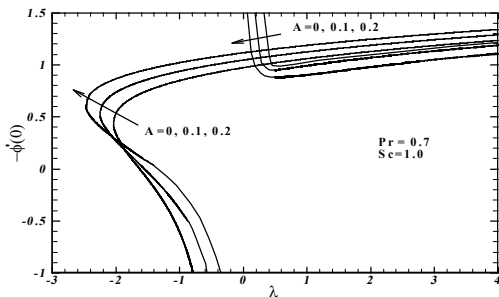


Figure 8. Variation of $-\phi'(0)$ with λ for different unsteadiness parameter A when $N=0.2$, $Pr = 0.7$, $Sc=1.0$ and case A.

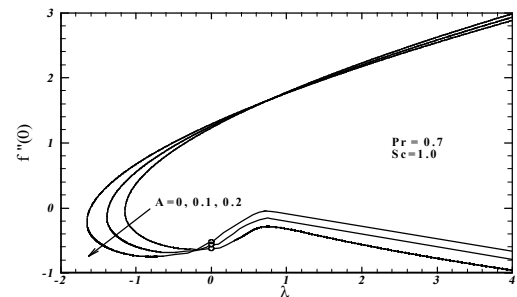


Figure 9. Variation of $f''(0)$ with λ for different unsteadiness parameter A when $N=0.2$, $Pr = 0.7$, $Sc=1.0$ and case B.

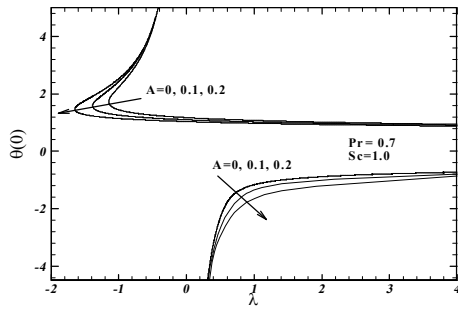


Figure 10. Variation of $\theta(0)$ with λ for different unsteadiness parameter A when $N=0.2$, $Pr = 0.7$, $Sc=1.0$ and case B.

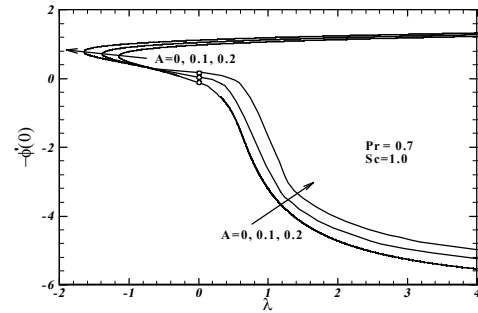
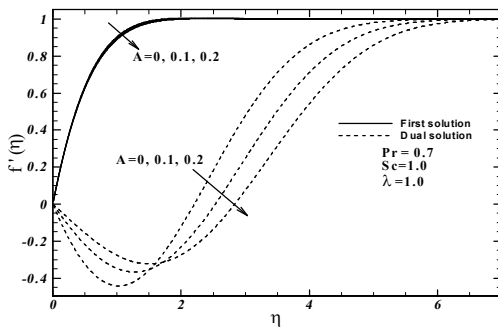
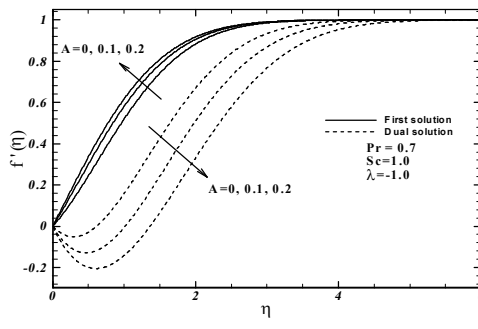


Figure 11. Variation of $-\phi'(0)$ with λ for different unsteadiness parameter A when $N=0.2$, $Pr = 0.7$, $Sc=1.0$ and case B.

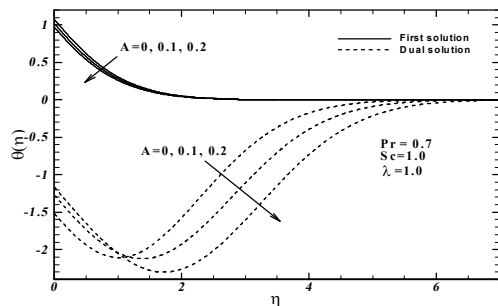


(a) Assisting flow

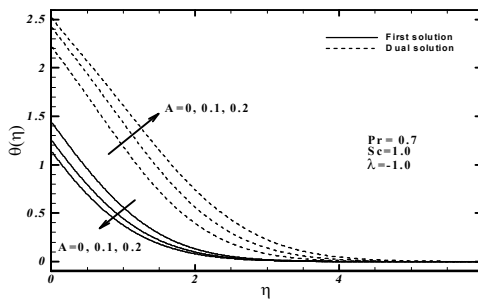


(b) Opposing flow

Figure 12. Velocity profiles $f'(\eta)$ for different unsteadiness parameter A when $Pr = 0.7$, $Sc=1.0$, $N=0.2$ (case B).

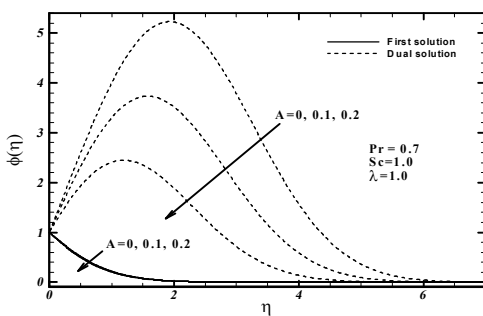


(a) Assisting flow

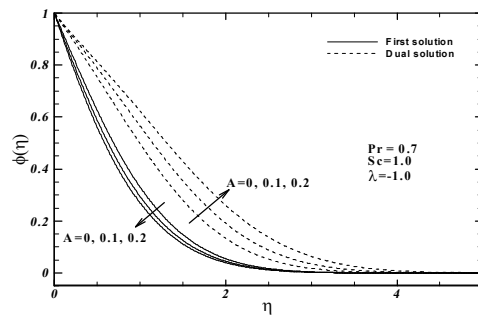


(b) Opposing flow

Figure 13. Temperature profiles $\theta(\eta)$ for different unsteadiness parameter A when $Pr = 0.7$, $Sc=1.0$, $N=0.2$ (case B).



(a) Assisting flow



(b) Opposing flow

Figure 14. Concentration profiles $\phi(\eta)$ for different unsteadiness parameter A when $Pr = 0.7$, $Sc=1.0$, $N=0.2$ (case B).

The effects of unsteadiness parameter A on the velocity, temperature and concentration profiles for case B are presented in Figures 12, 13 and 14, respectively. It is seen from these figures that the profiles for both first and second solutions satisfy the far field boundary conditions asymptotically, thus supporting the numerical results presented in Figures 9, 10 and 11. It can be seen that the profiles of the second solution have a much higher boundary layer thickness. In the first solutions, velocity profile for assisting flow and both of the temperature and concentration profiles for assisting and opposing flows decrease with the increasing of the unsteadiness parameter, while the velocity profile for opposing flow has an opposite trend. We also notice that the reversed flow near the wall is present for the second solutions in both of the assisting and opposing flows.

4. CONCLUSION

The problem of an unsteady mixed convection stagnation-point flow towards a permeable vertical plate with prescribed external flow immersed in an incompressible fluid was studied numerically. The governing partial differential equations were first transformed into a system of ordinary differential equations using a similarity transformation, before being solved numerically by a finite-difference scheme known as the fourth-order Runge–Kutta coupled with shooting technique. The effects of the unsteadiness parameter A , permeability parameter f_0 and the mixed convection parameter λ on the fluid flow and heat and mass transfer characteristics were discussed for two cases: prescribed surface temperature (case A) and prescribed surface heat flux (case B). The conclusions drawn from the study can be summarized as follows:

- Dual solutions exist for both assisting and opposing flows.
 - For the assisting flow case, a solution could be obtained for all positive values of λ , while for the opposing case, the solution terminated in a saddle-node bifurcation at $\lambda = \lambda_c$ ($\lambda_c < 0$).
 - As unsteadiness increases, the temperature and concentration profiles decrease for both of the prescribed surface temperature and heat flux.
- As expected, the mixed convection parameter increases the momentum, heat and mass transfer
- for the assisting flow case, while the opposite is true for the opposing case.
 - Suction at the wall increases the local skin friction parameter, the local heat and mass transfer parameters due to decreased thermal and concentration boundary layer thicknesses, while injection has an opposite effect.
 - Suction and unsteadiness widens the range of λ for

which the solution exists, while injection has opposite effects.

5. REFERENCE

1. Bejan, A., "Convection heat transfer, John Wiley & sons, (2013).
2. Incropera, F.P., "Fundamentals of heat and mass transfer, John Wiley & Sons, (2007).
3. Rogers, D.F., "Laminar flow analysis, Cambridge University Press, (1992).
4. Shu, J.-J. and Pop, I., "On thermal boundary layers on a flat plate subjected to a variable heat flux", *International Journal of Heat and Fluid Flow*, Vol. 19, No. 1, (1998), 79-84.
5. Risbeck, W., Chen, T. and Armaly, B.F., "Laminar mixed convection over horizontal flat plates with power-law variation in surface temperature", *International Journal of Heat and Mass Transfer*, Vol. 36, No. 7, (1993), 1859-1866.
6. Datta, P., Subhashini, S. and Ravindran, R., "Influence of surface mass transfer on mixed convection flows over non-isothermal horizontal flat plates", *Applied Mathematical Modelling*, Vol. 33, No. 3, (2009), 1285-1294.
7. Ishak, A., Nazar, R. and Pop, I., "The schneider problem for a micropolar fluid", *Fluid Dynamics Research*, Vol. 38, No. 7, (2006), 489-502.
8. Rahmannedzhad, J., Ramezani, A. and Kalteh, M., "Numerical investigation of magnetic field effects on mixed convection flow in a nanofluid-filled lid-driven cavity", *International Journal of Engineering-Transactions A: Basics*, Vol. 26, (2013), 1213-1224.
9. Rostamzadeh, A., Jafarpur, K., Goshtasbirad, E. and Doroodmand, M., "Experimental investigation of mixed convection heat transfer in vertical tubes by nanofluid: Effects of reynolds number and fluid temperature", *International Journal of Engineering-Transactions B: Applications*, Vol. 27, No. 8, (2014), 1251-1258.
10. De Hoog, F., Laminger, B. and Weiss, R., "A numerical study of similarity solutions for combined forced and free convection", *Acta Mechanica*, Vol. 51, No. 3-4, (1984), 139-149.
11. Afzal, N. and Hussain, T., "Mixed convection over a horizontal plate", *Journal of Heat Transfer*, Vol. 106, No. 1, (1984), 240-241.
12. Ramachandran, N., Chen, T. and Armaly, B.F., "Mixed convection in stagnation flows adjacent to vertical surfaces", *Journal of Heat Transfer*, Vol. 110, No. 2, (1988), 373-377.
13. Ridha, A. and Curie, M., "Aiding flows non-unique similarity solutions of mixed-convection boundary-layer equations", *Journal of Applied Mathematics and Physics*, Vol. 47, No. 3, (1996), 341-352.
14. Lok, Y.Y., Amin, N., Campean, D. and Pop, I., "Steady mixed convection flow of a micropolar fluid near the stagnation point on a vertical surface", *International Journal of Numerical Methods for Heat & Fluid Flow*, Vol. 15, No. 7, (2005), 654-670.
15. Deswita, L., Nazar, R., Ishak, A., Ahmad, R. and Pop, I., "Mixed convection boundary layer flow past a wedge with permeable walls", *Heat and Mass Transfer*, Vol. 46, No. 8-9, (2010), 1013-1018.
16. Merrill, K., Beauchesne, M., Previte, J., Paultet, J. and Weidman, P., "Final steady flow near a stagnation point on a vertical surface in a porous medium", *International Journal of Heat and Mass Transfer*, Vol. 49, No. 23, (2006), 4681-4686.
17. Ishak, A., Nazar, R., Arifin, N.M. and Pop, I., "Dual solutions in mixed convection flow near a stagnation point on a vertical porous plate", *International Journal of Thermal Sciences*, Vol. 47, No. 4, (2008), 417-422.

18. Ishak, A., Nazar, R. and Pop, I., "Dual solutions in mixed convection flow near a stagnation point on a vertical surface in a porous medium", *International Journal of Heat and Mass Transfer*, Vol. 51, No. 5, (2008), 1150-1155.
19. Subhashini, S., Samuel, N. and Pop, I., "Effects of buoyancy assisting and opposing flows on mixed convection boundary layer flow over a permeable vertical surface", *International Communications in Heat and Mass Transfer*, Vol. 38, No. 4, (2011), 499-503.
20. Subhashini, S., Samuel, N. and Pop, I., "Double-diffusive convection from a permeable vertical surface under convective boundary condition", *International Communications in Heat and Mass Transfer*, Vol. 38, No. 9, (2011), 1183-1188.
21. Merkin, J., "On dual solutions occurring in mixed convection in a porous medium", *Journal of Engineering Mathematics*, Vol. 20, No. 2, (1986), 171-179.
22. Harris, S., Ingham, D. and Pop, I., "Mixed convection boundary-layer flow near the stagnation point on a vertical surface in a porous medium: Brinkman model with slip", *Transport in Porous Media*, Vol. 77, No. 2, (2009), 267-285.
23. Postelnicu, A. and Pop, I., "Falkner–skan boundary layer flow of a power-law fluid past a stretching wedge", *Applied Mathematics and Computation*, Vol. 217, No. 9, (2011), 4359-4368.
24. Smith, F., "Steady and unsteady boundary-layer separation", *Annual Review of Fluid Mechanics*, Vol. 18, No. 1, (1986), 197-220.
25. White, F.M. and Corfield, I., "Viscous fluid flow, McGraw-Hill New York, Vol. 3, (2006).
26. Schlichting, H. and Gersten, K., "Boundary-layer theory, Springer Science & Business Media, (2000).
27. Yang, K.-T., "Unsteady laminar boundary layers in an incompressible stagnation flow", *Journal of Applied Mechanics*, Vol. 25, No. 4, (1958), 421-427.
28. Wang, C., "The unsteady oblique stagnation point flow", *Physics of Fluids*, Vol. 28, (1985), 2046-2049.
29. Rahimi, A.B. and Jalali, T., "Unsteady free convection from a sphere in a porous medium with variable surface temperature", *International Journal of Engineering-materials and Energy Research Center-*, Vol. 18, No. 4, (2005), 331-350.
30. Moghadam, A.J. and Rahimi, A.B., "A numerical study of flow and heat transfer between two rotating vertically eccentric spheres with time-dependent angular velocities", *International Journal of Engineering-Transactions A: Basics*, Vol. 21, No. 3, (2008), 295-318.
31. Haghighi, B. and Rahimi, A.B., "Effect of time-dependent transpiration on axisymmetric stagnation-point flow and heat transfer of a viscous fluid on a moving circular cylinder", *International Journal of Engineering-Transactions A: Basics*, Vol. 23, No. 3&4, (2010), 287-312.
32. Bachok, N., Ishak, A. and Pop, I., "The boundary layers of an unsteady stagnation-point flow in a nanofluid", *International Journal of Heat and Mass Transfer*, Vol. 55, No. 23, (2012), 6499-6505.
33. Rohni, A.M., Ahmad, S., Pop, I. and Merkin, J.H., "Unsteady mixed convection boundary-layer flow with suction and temperature slip effects near the stagnation point on a vertical permeable surface embedded in a porous medium", *Transport in Porous Media*, Vol. 92, No. 1, (2012), 1-14.
34. Ishak, A., Nazar, R., Bachok, N. and Pop, I., "Mhd mixed convection flow near the stagnation-point on a vertical permeable surface", *Physica A: Statistical Mechanics and its Applications*, Vol. 389, No. 1, (2010), 40-46.

Unsteady Heat and Mass Transfer Near the Stagnation-point on a Vertical Permeable Surface: a Comprehensive Report of Dual Solutions

H. Tamim, A. Abbassi

Department of Mechanical Engineering, Amirkabir University of Technology, Tehran, Iran

PAPER INFO

چکیده

Paper history:

Received 22 February 2013

Accepted in revised form 18 September 2014

Keywords:

Unsteady Flow
Double Diffusive Convection
Stagnation-point Flow
Mixed Convection
Dual Solutions
Vertical Surface
Suction/Injection

در این مقاله، مسئله جریان لایه مرزی جابجایی مرکب ناپایا از یک سیال تراکم ناپذیر لزج در مجاورت نقطه سکون بر روی یک صفحه نفوذپذیر عمودی به همراه هر دو حالت دمای دیواره و شار حرارتی دیواره مشخص به صورت عددی بررسی شده است. در اینجا، نیروهای شناوری هم‌سو و مخالف در نظر گرفته شده و بررسی شده‌اند. ابتدا معادلات دیفرانسیل جزئی غیرخطی حاکم بر میدان‌های جریان، حرارتی و غلظت با استفاده از یک مجموعه تبدیلات تشابهی مناسب به یک دستگاه معادلات دیفرانسیل معمولی کوپل تبدیل شد. دستگاه معادلات دیفرانسیل معمولی حاصل به صورت عددی به کمک تکنیک رانگ-کوتای ترکیب شده با روش شوتینگ حل گردید. نتایج عددی برای ضریب اصطکاک پوسته‌ای، عدد ناسلت و عدد شرود و نیز برای پروفیل‌های سرعت، دما و غلظت به ازای چندین مقدار پارامترهای به دست آمده به نام‌های پارامتر ناپایا بودن A ، پارامتر نفوذپذیری f_0 و پارامتر جابجایی مرکب λ به دست آمد. مشخص گردید که حل دوگانه برای هر دو جریان هم‌سو و مخالف وجود دارد و محدوده دارای پاسخ پارامتر جابجایی مرکب با مکش و پارامتر ناپایا افزایش می‌یابد.

doi: 10.5829/idosi.ije.2015.28.05b.16